Becker, K., Malone, M.J., et al., 1998
Proceedings of the Ocean Drilling Program, Initial Reports, Vol. 174B

1. INTRODUCTION[1]

Shipboard Scientific Party[2]

INTRODUCTION

In this chapter, we have assembled information that will help the reader understand the observations on which our preliminary conclusions are based. This information concerns only shipboard operations and analyses described in the site report in the Leg 174B *Initial Reports* volume of the *Proceedings of the Ocean Drilling Program*.

Authorship of Site Chapters

The separate sections of the site chapters were written by the following shipboard scientists (authors are listed in alphabetical order, no seniority is implied):

Site 395
Site Summary: Shipboard Scientific Party
Background and Objectives: Becker
Operations: Becker, Malone, Pollard
CORK/DVTP: Becker, Harris
Downhole Logging: Bartetzko, Goldberg, Pezard, Sun

Site 1074
Site Summary: Shipboard Scientific Party
Background and Objectives: Becker
Operations: Malone, Pollard
Lithostratigraphy: Arnold, Hurst
Paleomagnetism: Fuller
Inorganic Geochemistry: Malone
Physical Properties/Heat Flow: Harris, Matsumoto, Moran

CORK/DVTP

The primary objective of Leg 174B was to reenter Hole 395A for selected downhole logs, followed by installation of a Circulation Obviation Retrofit Kit (CORK) or long-term downhole hydrologic observatory. The logging program included deployments of the Davis-Villinger Temperature Probe (DVTP) and three Schlumberger logs that are described in the "Downhole Logging" section (this chapter). The techniques used for the DVTP and CORK were similar to those used during Legs 139, 164, and 168, when these tools were used to great advantage. These methods are described in the following publications:

1. DVTP: Shipboard Scientific Party (1996, 1997); and
2. CORK: Davis et al. (1992).

[1]Becker, K., Malone, M.J., et al., 1998. *Proc. ODP, Init. Repts.,* 174B: College Station, TX (Ocean Drilling Program).
[2]Shipboard Scientific Party is given in the list preceding the Table of Contents.

DOWNHOLE LOGGING

Introduction

Downhole logs may be used to determine the physical, chemical, and structural properties of formations penetrated by a drill hole. Wireline log data are rapidly collected using a variety of instruments that make continuous in situ measurements as a function of depth below the rig floor after the hole has been drilled (or reentered). Logs are essential to determine the borehole lithostratigraphy at a scale of investigation that links laboratory tests on core samples with regional geophysical studies. After processing, logs are typically displayed as curves or images of physical and chemical properties of the formations intersected by the borehole. Image logs, in particular, serve to illustrate the physical state of the hole and the character of the formations penetrated.

Data quality is largely determined by the state of the borehole wall. If it is irregular, wide, or there are many wash-outs, there may be problems with those tools that require good contact with the wall (density, porosity, and formation microscanner [FMS]). Deep investigation measurements such as resistivity and sonic velocity are least sensitive to borehole conditions. The quality of log data acquired in Hole 395A, which was drilled 21 yr before Leg 174B and may have several enlarged intervals, should be improved by utilizing deep investigation tools.

Operations

During ODP Leg 174B, Hole 395A was reentered and logged using three wireline tool strings (Table 1). The wireline tool strings combined standard Ocean Drilling Program (ODP) tools with two new tools, the azimuthal resistivity imager (ARI) and the dipole sonic imager (DSI). Standard logging tools, applications, and principles for marine geology and geophysics are described by Goldberg (1997) and in previous ODP *Initial Reports* volumes (e.g., Leg 172; Keigwin, Rio, Acton, et al., 1998). A description of the ARI and DSI tools used during Leg 174B is given below. The wireline tools and the shipboard multi-tasking acquisition and imaging system (MAXIS) unit, which recorded and monitored the log data acquisition in real time, were provided by Schlumberger. The Lamont-Doherty Earth Observatory-Borehole Research Group (LDEO-BRG) active wireline heave compensator was also used to minimize the effect of the ship's motion during each of the three logging tool runs. After the logs were acquired, the data were transferred to the Downhole Measurement Lab for preliminary interpretation using the GeoFrame software and also to LDEO-BRG for processing using the SeaNET high-speed satellite data link.

Dipole Sonic Imager

Applications/Operations

The DSI tool employs a combination of monopole and dipole transducers to make accurate measurements of sonic wave propagation in a wide variety of lithologies (Schlumberger, 1995). In addition to a robust and high-quality measurement of compressional-wave ve-

Table 1. Order and specification of the downhole tool strings deployed during Leg 174B.

Tool string	Tool	Measurement	Sample interval (cm)	Approximate vertical resolution (cm)
Run 1- DVTP	DVTP	Temperature	2000	—
Run 2- ARI (total length ~22 m)	HNGS*	Natural gamma	15	45
	ARI*	Azimuthal resistivity	15	15/60
	GPIT*	Magnetic orientation	0.25	0.5
	TLT	Temperature	1 per s	—
Run 3-FMS-sonic (total length ~33 m)	NGT*	Natural gamma	15	45
	DSI*	Dipole sonic	15	120
	GPIT*	Magnetic orientation	0.25	0.5
	FMS*	Microresistivity image	0.25	0.5
Run 4-triple combo (total length ~32 m)	HNGS*	Natural gamma	15	45
	APS*	Porosity	5 or 15	30
	LDS*	Bulk density, PEF	2.5 or 15	15/45
	DITE*	Resistivity	2.5 or 15	200/150/75
	GPIT*	Magnetic orientation	0.25	0.5

Notes: * = trademarks of Schlumberger. DVTP = Davis-Villinger Temperature Probe, HNGS = hostile-environment natural gamma-ray spectrometry sonde, ARI = azimuthal resistivity imager, GPIT = three-axis magnetometer-inclinometer logging tool, TLT = temperature-logging tool, NGT = natural-gamma spectrometry tool, DSI = dipole sonic imager, FMS = formation microscanner logging tool, APS = advanced porosity sonde, LDS = lithodensity sonde, and DITE = digital induction tool. PEF = photoelectric factor.

locity, the DSI excites a flexural mode in the borehole that can be used to determine shear-wave velocity in all types of formations. When the formation shear velocity is less than the borehole fluid velocity, particularly in unconsolidated sediments, the flexural wave travels at the shear-wave velocity and is the most reliable way to estimate a shear velocity log. The configuration of the DSI also allows recording of cross-line dipole waveforms. These modes can be used to estimate shear-wave splitting caused by preferred mineral and/or structural orientations in consolidated formations. A low-frequency source enables Stoneley waveforms to be acquired as well.

The deployment of the DSI generally consists of two passes in the FMS-Sonic tool string combination, where the DSI replaces the more commonly used array sonic digital logging tool (SDT). Two passes are required to obtain consistent azimuth measurements for the cross-dipole mode and to acquire additional recording modes at normal logging speeds. Switching between recording modes was accomplished while the tool was downhole. The DSI was run first using the conventional *P*-wave first arrival, in-line dipole, and cross-dipole recording modes; then subsequently using the Stoneley-wave, high-frequency *P*- and *S*-wave, and cross-dipole recording modes.

Tool Configuration

The DSI tool is divided into a transmitter sonde, a receiver sonde, and an acquisition cartridge (Fig. 1). The transmitter sonde consists of a power amplifier and switching circuitry, which drive one dual-frequency (14 and 1 kHz) monopole transmitter and two pairs of dipole (2.2 kHz) transmitters. Separate source functions with appropriate shape and frequency content are used for compressional-, Stoneley-, and dipole-wave modes, respectively.

The receiver sonde houses an array of eight receiver groups with 15-cm spacing, each consisting of four orthogonal elements that are aligned with the dipole transmitters. During acquisition, the output from these 32 individual elements are differenced or summed appropriately to produce in-line and cross-line dipole signals or monopole-equivalent (compressional and Stoneley) waveforms. A first generation DSI tool was deployed during ODP Legs 149 and 150, although only in-line shear waveforms were recorded. The reader is referred to the ODP *Initial Reports* volumes of these legs for more information regarding these experiments (cf. Sawyer, Whitmarsh, Klaus, et al., 1994; Mountain, Miller, Blum, et al., 1994).

Data Processing

Preliminary processing of DSI data is accomplished by MAXIS to estimate monopole- and dipole-mode velocities using waveform correlation of the digital signals recorded at each receiver. In most instances, the shear-wave data should be reprocessed postcruise to correct for the effects of dispersion, which is caused by the variation of sound velocity with frequency. Often in dipole-mode propagation, the flexural wave is dispersive; for monopole-mode propagation, the Stoneley wave is dispersive. Processing techniques must be applied to account for a dispersive model without assumptions or to compute a bias correction to minimize any frequency effects on the velocity.

In addition, information such as mode amplitudes, shear-wave polarization, and Poisson's ratio can be extracted postcruise to provide information about lithology, porosity, and anisotropy. Amplitude processing and stacking of Stoneley-wave reflections may also be used to identify fractures, fracture permeability, and aperture in the vicinity of the borehole.

Azimuthal Resistivity Imager

Applications/Operations

The ARI is a combination of two different downhole sensors; a standard DLL tool and a multi-electrode cylindrical array that makes 12 directional measurements of electrical resistivity around the borehole, also based on the laterolog principle (Schlumberger, 1993). Similar to the FMS, the ARI produces images of layering and of structures that intersect the borehole, but with coarser vertical resolution and complete azimuthal coverage. Whereas FMS electrodes are pad-mounted and in contact with the borehole surface, the ARI provides a remote image of the formation in a similar way to that of the borehole televiewer downhole tool (BHTV). The ARI electrodes measure deep and shallow readings to fully correct the azimuthal resistivities for changes in borehole size.

The ARI tool may be deployed (1) in combination with the triple combo tool string, where it replaces the more commonly used digital induction tool (DITE); (2) in several other combinations; or (3) independently. However, the ARI must be used with the three-axis magnetometer-inclinometer logging tool (GPIT) for image orientation, as used for the FMS tool. Repeat passes of the ARI may be useful to obtain consistent azimuth measurements.

Tool Configuration

The ARI electrode array operates at 35 Hz for the deep readings and focuses currents that flow from the 12 electrodes to the grounded logging cable (Fig. 2). The sum of these 12 readings produces a high-resolution measurement, equivalent to a single laterolog electrode of the same height. To correct for tool eccentralization and variations in borehole shape, a shallow auxiliary measurement of electrical resistivities is performed at a much higher frequency of 71 kHz. This measurement responds primarily to the volume of borehole fluid affecting each electrode. If the borehole fluid resistivity is independently measured, then borehole size and shape can be deduced from the auxiliary array measurements. Whereas the vertical resolution of the standard laterolog readings is ~0.60 m, the high-resolution array can

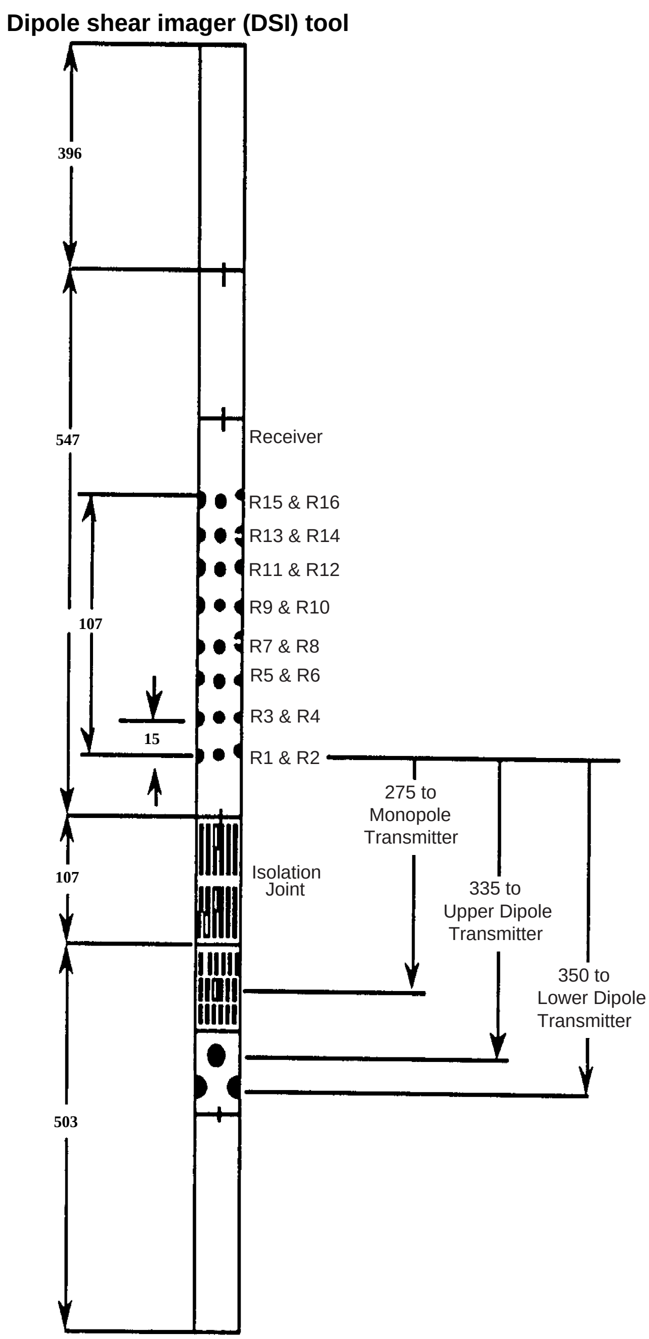

Figure 1. Diagram showing the DSI tool configuration used during Leg 174B (after Schlumberger, 1995). Distances are given in centimeters. The DSI tool is divided into a transmitter sonde, a receiver sonde, and an acquisition cartridge. The transmitter sonde drives one dual-frequency (14 and 1 kHz) monopole transmitter and two pairs of dipole (2.2 kHz) transmitters. The receiver sonde houses an array of eight receiver groups with 15-cm spacing, each consisting of four orthogonal elements that are aligned with the dipole transmitters. The output from these 32 individual elements are differenced or summed to produce in-line and cross-line dipole signals or monopole-equivalent (compressional and Stoneley) waveforms, respectively.

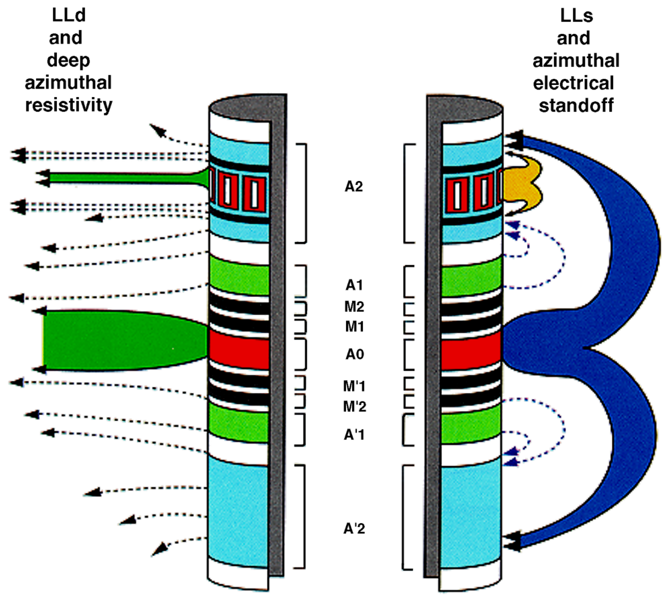

Figure 2. Diagram illustrating the ARI electrode geometry used during Leg 174B and the standard electrode array for the DLL resistivity measurements (after Schlumberger, 1993). The azimuthal array for imaging is included as part of the "A2" electrode of the DLL; the deep currents return to the base of the drill pipe in the ODP experimental configuration. Both LLd and deep azimuthal resistivity measurements are performed at a frequency of 35 Hz. Shallow azimuthal measurements are used to compute the electrical signal coming from the borehole and subtracted from the deep azimuthal measurements to correct for tool eccentering. This measurement is performed at high frequency (71 kHz).

reduce this by up to a factor of 6, depending on the formation resistivity.

Data Processing and Interpretation

Preliminary processing of ARI images may be accomplished using GeoFrame in a similar manner to FMS image processing. Comparison of image data from different logging tools can also be displayed using this software, which may provide information about fracture and fault orientation and aperture, formation dip and heterogeneity, and borehole shape. Because the ARI is less sensitive to features near the borehole than the FMS, such as drilling-induced fractures, the origin and lateral extent of such effects may be determined from the comparison of FMS and ARI images.

LITHOSTRATIGRAPHY

This section outlines the procedures followed to document the basic sedimentology of the cores recovered on Leg 174B, including core description, X-ray diffraction (XRD), and smear-slide preparation. Only general procedures are outlined, except where they depart significantly from ODP conventions.

Visual Core Description

Barrel Sheets

Information from megascopic description of each core was directly entered into AppleCORE (v0.7.5e) software, which generates a simplified, one-page graphical description of each core (barrel sheet). Barrel sheets are presented with whole-core photographs in the "Cores" section, this volume.

The lithology of the recovered material is represented on barrel sheets by ornaments in the column entitled "Graphic Lithology" (Fig.

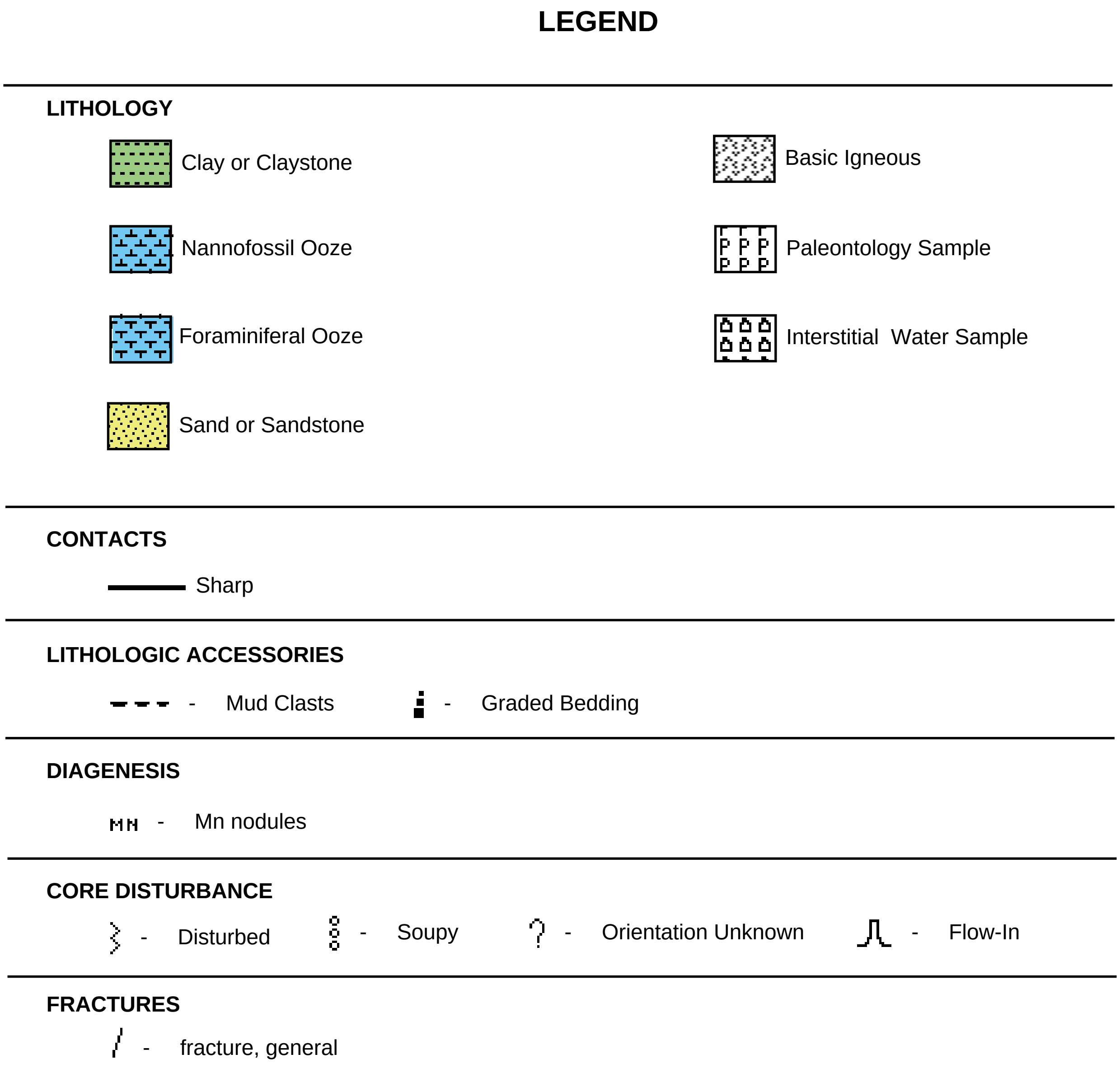

Figure 3. Key to ornaments and symbols used to represent lithology, sedimentary structures, diagenetic components, and drilling disturbance in the barrel

3). The sediments recovered from Site 1074 contain nannofossil ooze with variable amounts of clay, foraminifers, and radiolarians. Grain-size divisions for sand, silt, and clay are those of Wentworth (1922). Sediment with a lithologic component >10% is normally plotted as a vertical strip within the Graphic Lithology column, with the implication that the component is dispersed in the coexisting sediment. Constituents accounting for <10% of a given lithology or a stratigraphic interval (or others remaining after the representation of the three most abundant lithologies and components) are not shown in the Graphic Lithology column, but are indicated in the "Remarks" section of the barrel sheet.

A wide variety of features that characterize the sediment, such as primary sedimentary structures, bioturbation parameters, soft-sediment deformation, and structural and diagenetic features, are indicated in columns to the right of the graphic log. A key to the full set of symbols used on the graphic sedimentologic columns is shown in Figure 3.

Deformation and disturbance of sediment that clearly resulted from the coring process are illustrated in the Drilling Disturbance column, using symbols shown in Figure 3. Blank regions indicate the absence of coring disturbance.

A summary lithologic description with sedimentologic highlights is given in the Remarks column of the barrel sheet. This generally consists of two parts: (1) a section that lists all the major sediment lithologies; and (2) an extended summary description of the sediments, including composition, sedimentary structures, and other notable characteristics. Descriptions and locations of thin, interbedded, or minor lithologies that could not be depicted in the Graphic Lithology column are presented in the Remarks column where space permits.

Sediment Classification

The sediment classification scheme used during Leg 174B is descriptive and is largely the same as in previous ODP legs (Fig. 4). Composition and texture are the only criteria used to define lithology. Genetic terms such as pelagic, hemipelagic, turbidite, debris flow, etc., do not appear in this classification. The term "clay" is used for

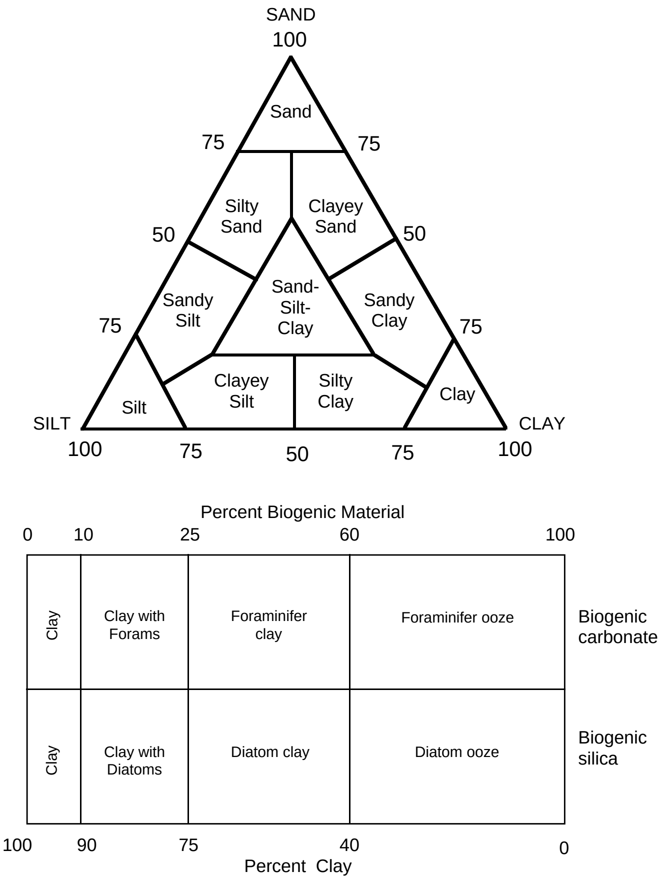

Figure 4. Textural classification scheme for siliciclastic sediments (top) and the procedure for naming mixtures of biogenic and siliciclastic materials (bottom). The textural classification scheme is from Shepard (1954). The sand-, silt-, and clay-sized fractions are defined using the Wentworth (1922) grade scale. The names used on the Shepard triangle are the same as shown in Figure 3. In the scheme for biogenic-siliciclastic mixtures, the names for microfossil components and the siliciclastic fraction are examples only (i.e., place-holders) and can be replaced by any valid textural name (for siliciclastic fraction) or microfossil name.

both clay minerals and other siliciclastic material <4 µm in size. Biogenic components are not described in textural terms. Thus, a sediment with 55% sand-sized foraminifers and 45% siliciclastic clay is called a foraminifer clay, not a foraminifer clayey sand.

The principal name is determined by the component or group of components (e.g., total biogenic carbonate) that comprise(s) at least 60% of the sediment or rock, except for subequal mixtures of biogenic and nonbiogenic material. If the total of a nonbiogenic component is >60%, the main name is determined by the relative proportions of sand, silt, and clay sizes when plotted on a Shepard (1954) classification diagram (Fig. 4). Examples of nonbiogenic principal names are clay, silt, silty clay, or sand. If the total of biogenic components is greater than 60%, the principal name is ooze.

In mixtures of biogenic and nonbiogenic material where the biogenic content is 25%–60%, the principal name consists of two parts: (1) the name of the major fossil(s), hyphenated if necessary with the least common fossil listed first, followed by (2) the textural name appropriate for the siliciclastic components.

Ichnology

Ichnologic analysis included evaluation of the extent of bioturbation. To assess the degree of bioturbation semiquantitatively, a modified version of the Droser and Bottjer (1991) ichnofabric index (ii) scheme was employed (e.g., ii1 = barren or no bioturbation; ii5 = abundant bioturbation or completely bioturbated). These indices are illustrated using color-banded symbols in the "Relative Bioturbation" column of the barrel sheets.

Igneous Rocks

The final core recovered from Site 1074 contained mainly aphyric basalt, which is represented by the AppleCORE pattern and code for Basic-Igneous rock because AppleCORE at present is primarily a sedimentary rock description tool and the codes available for igneous rocks are very limited. The whole of the rock description is contained in the "Remarks" section of the barrel sheet for the core. The few features that characterize the igneous rocks in the core, such as fractures and core orientation, are indicated in columns to the right of the graphic log (Fig. 3). No attempt was made to indicate the size or position of the pieces in the section because of the relatively simple lithology, lack of important orientation information, and small amount of rock recovered.

Summary Graphic Columns

Graphic sedimentologic columns are presented in the "Lithostratigraphy" section of each site chapter and are based on the information compiled from the barrel sheets. The columns show lithology, grain-size variation, and sedimentary structures.

X-ray Diffraction

Relative abundances of the main silicate and carbonate minerals were determined semiquantitatively using a Philips model PW-1729 X-ray diffractometer with Cu Kα radiation (Ni filter). Each bulk-sediment sample was freeze dried, crushed, and mounted with a random orientation into an aluminum sample holder. Instrument conditions were as follows: 40-kV, 35-mA, goniometer scan from 2° to 70° 2θ for bulk samples, step size 0.01° 2θ, scan speed at 1.2° 2θ/min, and count time 0.5 s. Peak intensities were converted to values appropriate for a fixed-slit width. Relative abundances of various minerals were established on the basis of integrated peak intensity. Ratios and relative abundances reported in this volume are useful for general characterization of the sediments, but should not be viewed as precise quantitative data.

Smear Slides

Petrographic analysis of the sediment was primarily by smear-slide description. We emphasize here that smear-slide analysis provides only crude estimates of the relative abundances of detrital constituents, and therefore these data are not presented in a table, but only used to classify the sediment. The mineral identification of finer grained particles is difficult using only a binocular microscope, and sand-sized grains tend to be underestimated because they cannot be incorporated into the smear evenly.

PHYSICAL PROPERTIES

Introduction

Shipboard measurements of physical properties aid in the characterization of lithologic units and help correlate core lithology, downhole geophysical logs, and seismic data.

Magnetic susceptibility, bulk density, and compressional-wave velocity were measured in whole-round core sections on the multisensor track (MST). Thermal conductivity measurements using the needle probe method were performed at discrete intervals, also in whole-round sections. Samples were taken at regularly spaced intervals. Blum (1997) gives detailed descriptions of most of the techniques used. A few additional measurements of discrete compressional-wave velocity, shear strength, and electrical resistivity were made on selected core intervals to test the database and to assess the resistivity probe and methods. These data are not included in the initial results.

Multisensor Track

Core sections were run through the MST after they had warmed up to at least 18°C (measured at the top of the section). The gamma-ray attenuation porosity evaluator (GRAPE) measured bulk density at a 1-cm interval by comparing the attenuation of gamma rays through the cores with attenuation through aluminum and distilled water calibration standards. The *P*-wave logger (PWL) transmits a 500-kHz compressional-wave pulse through the core. The transmitting and receiving transducers are aligned perpendicular to the long axis of the core (z-direction). A pair of displacement transducers monitors the separation between the compressional-wave transducers. As with the GRAPE sensor, measurements were taken at a 1-cm interval. Calibration of the displacement transducer and measurement of electronic delay within the PWL circuitry were carried out using a series of acrylic blocks of known thickness and *P*-wave traveltime. The validity of the calibration was checked by measuring the *P*-wave velocity through a section of liner filled with distilled water. Magnetic susceptibility was measured on all sections at a 1-cm interval using the Bartington meter (model MS2C), which has an 80-mm internal-diameter loop. Natural gamma-ray (NGR) emission was measured at 20-cm intervals in one section as a test of the database; these data are not included as part of the initial results.

Thermal Conductivity

Thermal conductivity is the measure of a material's ability to transmit heat by molecular conduction. Thermal conductivity of soft sediment was measured using the needle probe method, in full-space configuration (Von Herzen and Maxwell, 1959). One measurement every other section was made using a single-probe Teka (Berlin) TK-04 unit after the cores had equilibrated to laboratory temperature. Thermal conductivity measurements were made near the middle of cores on which the Adara temperature tool had been run. Data are reported in units of W/(m·K).

A needle probe (#V00894) containing a heater wire and a calibrated thermistor was inserted into the sediment through a small hole drilled in the core liner, usually near the center of the section, before core splitting. Three measuring cycles were automatically carried out at each location. At the beginning of each test, a self test, which included a drift study, was conducted. Once the samples were equilibrated, the heater circuit was closed, and the temperature rise in the probes was recorded. Thermal conductivities were calculated from the rate of temperature rise while the heater current was flowing.

Temperatures measured ~150 s from the beginning of the run were fit to an approximation of the solution of a constantly heated line source (Kristiansen, 1982; see Blum [1997] for details). Errors are between 5% and 10%. Corrections were not attempted for in situ temperature or pressure effects. Measurements accompanied during processing by "high drift" or "high error" messages were discarded before plotting results.

Temperature

Downhole temperature measurements were made in Hole 1074A with the Adara tool. This was deployed in the APC-coring shoe as part of regular coring operations. The components of the Adara tool are contained in the annulus within the coring shoe and include a platinum temperature sensor and a data logger. The platinum resistance temperature device (RTD) is calibrated over a range of –20° to 100°C, with a resolution of 0.01°C. In operation, the coring shoe was mounted on a core barrel and lowered down the pipe by wireline. The tool was typically held for 5–10 min at the mudline to equilibrate with bottom-water temperature and then lowered to the end of the drill string. Standard APC-coring techniques were used, with the core barrel being fired out through the drill bit using hydraulic pressure. The Adara tool is then left in the sediment for 10–15 min, ~9.5 m ahead of the bit, to obtain a temperature record. This provided a sufficiently long transient record for a reliable extrapolation of the steady-state temperature. The nominal accuracy of the unreduced temperature measurement is estimated to be 0.1°C.

Index Properties

Index properties (bulk density, grain density, water content, porosity, dry density, and void ratio) were calculated from measurements of wet and dry masses and wet volumes. Index property samples of ~10 cm^3 were usually taken at the locations of velocity and resistivity measurements. Sample frequency was two to three per core.

Sample mass was determined using a Scitech electronic balance. The sample mass was counterbalanced by a known mass, such that only mass differences of usually <2 g were measured. The balance was also equipped with a computer averaging system that corrected for ship accelerations. Dry mass was measured from samples oven dried at 110°C ± 5°C for 24 hr and cooled in a desiccator for 2 hr.

Wet volumes were determined using a Quantachrome Penta-Pycnometer; a helium-displacement pycnometer, for two samples; and a constant volume sampler for the remaining samples. In the Penta-Pycnometer sample, volumes were repeated up to three times until the last three measurements had <0.01% standard deviation. A purge time of 1 min was used before each run. A reference sphere of known volume was run with each group of four samples during all of the measurements. The standard was rotated systematically among cells to check for errors.

Water content, bulk density, porosity, grain density, dry density, and void ratio were determined following procedures outlined in Blum (1994), which comply with the American Society for Testing and Materials (ASTM) designation (D) 2216 (ASTM, 1989). Bulk density, grain density, and porosity were computed from the wet and dry masses of the sample and dry volume using Methods B and A of Blum (1994). Calculated values include correction for salt, assuming a pore-water salinity of 35 g/L (Boyce, 1976).

INORGANIC GEOCHEMISTRY

Shipboard interstitial water analyses were performed on water squeezed from whole-round sections (Manheim and Sayles, 1974). Standard precautions were taken during handling, processing, and extraction (e.g., Mountain, Miller, Blum, et al., 1994). Chloride, salinity, alkalinity, pH, sulfate, and dissolved silica were analyzed according to the methods described in ODP Technical Note No. 15 (Gieskes et al., 1991). Ammonium determinations were attempted, but concentrations were near or below detection limits. Potassium, calcium, and magnesium were analyzed by ion chromatography using a DX-100 ion chromatograph fitted with a CS12 column. Strontium was analyzed by atomic absorption spectroscopy using an air/nitrous oxide flame and 1% lanthanum as an ionization suppressor. The precisions of the methods are given in Table 2.

REFERENCES

ASTM, 1989. *Annual Book of ASTM Standards for Soil and Rock: Building Stones* (Vol. 4.08): *Geotextiles:* Philadelphia (Am. Soc. Testing and Mater.).

Blum, P., 1994. *Index Properties: ODP Shipboard Laboratory Manual*, Version 155, College Station, TX (Ocean Drilling Program).

————, 1997. Physical properties handbook: a guide to the shipboard measurement of physical properties of deep-sea cores. *ODP Tech. Note, 26*.

Boyce, R.E., 1976. Definitions and laboratory techniques of compressional sound velocity parameters and wet-water content, wet-bulk density, and porosity parameters by gravimetric and gamma-ray attenuation techniques. *In* Schlanger, S.O., Jackson, E.D., et al., *Init. Repts. DSDP,* 33: Washington (U.S. Govt. Printing Office), 931–958.

Davis, E.E., Becker, K., Pettigrew, T., Carson, B., and MacDonald, R., 1992. CORK: a hydrologic seal and downhole observatory for deep-ocean boreholes. *In* Davis, E.E., Mottl, M.J., Fisher, A.T., et al., *Proc. ODP, Init. Repts.,* 139: College Station, TX (Ocean Drilling Program), 43–53.

Droser, M.L., and Bottjer, D.J., 1991. Trace fossils and ichnofabric in Leg 119 cores. *In* Barron, J., Larsen, B., et al., *Proc. ODP, Sci. Results,* 119: College Station, TX (Ocean Drilling Program), 635–641.

Gieskes, J.M., Gamo, T., and Brumsack, H., 1991. Chemical methods for interstitial water analysis aboard *JOIDES Resolution. ODP Tech. Note,* 15.

Goldberg, D., 1997. The role of downhole measurements in marine geology and geophysics. *Rev. Geophys.,* 35:315–342.

Keigwin, L.D., Rio, D., Acton, G., et al., 1998. *Proc. ODP, Init. Repts*., 172: College Station, TX (Ocean Drilling Program).

Kristiansen, J.I., 1982. The transient cylindrical probe method for determination of thermal parameters of earth materials [Ph.D. dissert.]. Aaehus Univ.

Manheim, F.T., and Sayles, F.L., 1974. Composition and origin of interstitial waters of marine sediments, based on deep sea drill cores. *In* Goldberg, E.D. (Ed.), *The Sea* (Vol. 5): *Marine Chemistry: The Sedimentary Cycle:* New York (Wiley), 527–568.

Mountain, G.S., Miller, K.G., Blum, P., et al., 1994. *Proc. ODP, Init. Repts.,* 150: College Station, TX (Ocean Drilling Program).

Sawyer, D.S., Whitmarsh, R.B., Klaus, A., et al., 1994. *Proc. ODP, Init. Repts.,* 149: College Station, TX (Ocean Drilling Program).

Schlumberger, 1993. *ARI—Azimuthal Resistivity Imager:* (Schlumberger Wireline and Testing), SMP-5160.

Schlumberger, 1995. *DSI—Dipole Sonic Imager:* (Schlumberger Wireline and Testing), SMP-5128.

Shepard, F., 1954. Nomenclature based on sand-silt-clay ratios. *J. Sediment. Petrol.,* 24:151–158.

Shipboard Scientific Party, 1996. Explanatory notes. *In* Paull, C.K., Matsumoto, R., Wallace, P.J., et al., *Proc. ODP, Init. Repts.,* 164: College Station, TX (Ocean Drilling Program), 13–41.

————, 1997. Explanatory notes. *In* Davis, E.E., Fisher, A.T., Firth, J.V., et al., *Proc. ODP, Init. Repts.,* 168: College Station, TX (Ocean Drilling Program).

Von Herzen, R.P., and Maxwell, A.E., 1959. The measurement of thermal conductivity of deep-sea sediments by a needle-probe method. *J. Geophys. Res.,* 64:1557–1563.

Wentworth, C.K., 1922. A scale of grade and class terms of clastic sediments. *J. Geol.,* 30:377–392.

Ms 174BIR-101

Table 2. Relative standard deviations for the methods used during Leg 174B.

Parameter	SD (%)	Sample type
Cl^-	0.1	IAPSO
Alkalinity	2.8	IAPSO
SO_4^{2-}	2.1	IAPSO
K^+	1.6	IAPSO
Mg^{2+}	1.3	IAPSO
Ca^{2+}	3.4	IAPSO
Sr^{2+}*	0.9	IAPSO
H_4SiO_4*	0.5	Standard curve (100–1000 µM)

Notes: SD = standard deviation. IAPSO = International Association for the Physical Sciences of the Ocean. * = the reported precisions for Sr^{2+} and H_4SiO_4 are based on triplicates analyses of the entire procedure, however, the extremely low precisions are likely somewhat higher for these techniques.